Study of the Adsorption Layer at the Glass-Dye Solution Interface by Variable Incidence-Angle Internal-Reflection Spectrometry

Teruo HINOUE,* Goro IMAMURA, and Yu YOKOYAMA
Department of Chemistry, Faculty of Science, Osaka University, 1-1 Machikaneyama, Toyonaka, Osaka 560
(Received July 21, 1993)

The reflectivity was measured at the interface between the glass substrate and the Brilliant Blue (BB) or Methylene Blue (MB) aqueous solution as a function of the angle of incidence at 632.8 nm from a He–Ne laser. The relationship between the reflectivity and the angle of incidence was analyzed by an approximate expression derived from the basic theory of internal reflection spectroscopy. On the other hand, a plot of the reflectivity against the effective thickness was used as a ready diagnosis of the dye adsorbed by the glass substrate. From the results it has been suggested that BB is not adsorbed, whereas MB is. Based on a parameter obtained experimentally, the thickness of the adsorption layer was determined to be 0.65±0.18 nm. This result suggests that the MB cation is adsorbed parallel to the glass surface to form a monomolecular layer. Further, it has been revealed from a similar analysis that the addition of a cationic surfactant with a long alkyl chain in the MB solution prevents the adsorption of MB by the glass substrate, whereas the addition of an anionic surfactant with a long alkyl chain promotes adsorption.

A solid–liquid interface has been widely utilized in analytical chemistry as a reaction field at which chemical species of interest can be determined or are separated through specific interfacial phenomena, such as electrolysis, ion exchange and adsorption/desorption. Various optical techniques have therefore been proposed and developed for observing the interface *in situ*, especially in the field of electrochemistry.[1—5] We have developed an internal-reflection spectrometry for examining the concentration depth profile of a light-absorbing species at a glass-solution interface, bearing in mind the ability of *in situ* observations of the interface, the high spatial resolution on the order of nm, and the instrumental convenience for experiments,[6—8] and have combined it with photoacoustic detection.[9—12] In internal-reflection spectrometry, a change in the angle of incidence above the critical angle leads to change in the penetration depth, that is, a change in the sampling depth in the solution away from the interface. When the solution contains a light-absorbing species, such as a dye, the light is absorbed through the evanescent wave emerging from the glass surface into the solution and, consequently, the reflectivity is reduced. It is well known that the relationship between the reflectivity and the concentration depth profile is expressed by a Laplace transformation using the penetration depth as variable.[13] Therefore, a mathematical treatment by an inverse Laplace transformation allows a determination of the concentration depth profile.[12,14,15] However, this mathematical treatment is not applicable to an analysis of the interface, unless the solution region near to the interface has practically the same refractive index as does the bulk of the solution. It is therefore difficult to apply it to the analysis of any interface at which an optically different phase, such as an adsorption layer, is present. The present paper describes a novel treatment for analyzing such an interface with the adsorption layer by a few approximate expressions derived from the basic theory of internal-reflection spectroscopy. The analysis was applied to interfaces with an without an adsorption layer.

Experimental

Apparatus. Figure 1 shows the experimental arrangement for measuring the reflectivity at the glass-dye solution interface as a function of the angle of incidence. A He–Ne laser (Spectra Physics, 105-1) was operated at 632.8 nm with a nominal power of 10 mW. The probe beam from the laser was chopped at 130 Hz by an optical chopper. The intermittent beam was separated into two beams by a beam splitter. One beam was directed toward the photodiode detector for monitoring the fluctuation in the laser power, whereas the other beam was directed toward a cell located on the inner stage of the goniometer for measuring the reflectivity through a convex lens with a focal length of 300 mm and a polarizer. The reflected beam from the glass-solution interface was detected by a photodiode detector attached to the outer stage of the goniometer. The outputs from the photodiode detectors were amplified by lock-in amplifiers (NF,

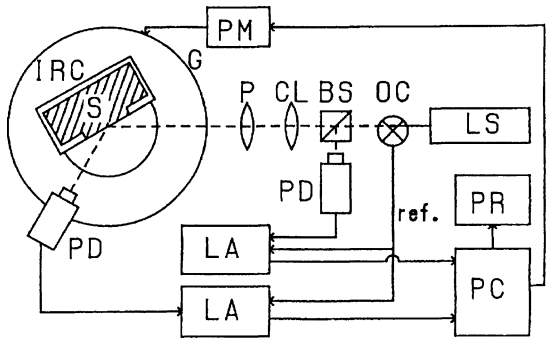

Fig. 1. Experimental arrangement for variable incidence-angle internal-reflection spectrometry. LS, He–Ne laser; OC, Optical chopper; BS, Beam splitter; CL, Convex lens; P, Polarizer; PM, Pulse motor; G, Goniometer; IRC, Internal reflection cell; S, Dye solution; PD, Photodiode detector; LA, Lock-in amplifier; PC, Personal computer; PR, Printer.

LI-574A and LI-574). A reference signal was supplied from the optical chopper. The signal intensity from each lock-in amplifier and the angle of incidence were registered on a personal computer through an A/D converter. Setting the angle of incidence was performed by rotating the goniometer with the pulse motor controlled by the personal computer.

Figure 2 shows an exploded view of the cell used. The cell was machined from a polychloroetylene trifluoride resin block; a hole of 8 mm in diameter was drilled in its front plane. A semicylindrical prism made of glass (BK 7, $n=$ 1.515 at 632.8 nm) was fixed on the front plane of the cell by two binders so that the hole was blocked by the bottom plane of the prism. Thus, the solution in the cell was in contact with the bottom plane of the prism to form a glass-solution interface.

Determination of the Reflectivity. Before any measurement, the bottom surface of the glass prism was kept in touch with the solution until the signal of the reflected beam attained a constant intensity so as to equilibrate the interface. After a measurement, each signal intensity of the reflected beam was normalized by the corresponding signal intensity for the laser power in order to eliminate any effect due to the fluctuation of the laser power. In addition, polarized light perpendicular to the plane of incidence was used in all of the measurements.

At first, the normalized signal intensities were measured at a series of angles of incidence for the glass-distilled water interface. On the other hand, the calculated reflectivities were obtained at the same angles of incidence by using the optical parameters of water (n=1.332 at 632.8 nm) and the glass prism. Then, a correction factor was determined at each angle of incidence as the ratio of the normalized signal intensity and the calculated reflectivity. Next, the normalized signal intensities were measured at the same angles of incidence for the glass-dye solution interface, and were corrected with the corresponding previously determined correction factors. Thus, the reflectivity was determined at each angle of incidence for the glass-dye solution interface.

Reagents. Brilliant Blue FCF (BB) and Methylene Blue (MB) supplied by Tokyo Kasei Kogyo Co., Ltd. were used without further purification. All chemicals serving as a cationic or an anionic surfactant were of reagent grade. The dye solutions were prepared with distilled water. The concentrations of the dye and the surfactant were 1.0 mmol dm^{-3} and 0.2 mmol dm^{-3}, and pH's of all dye solutions were between 4 and 6. Before each measurement, the glass prism was ultrasonically rinsed with methanol in order to remove MB adsorbed by the glass prism and finally rinsed with distilled water. The prism was dried at room temperature and was stored in a desiccator until used.

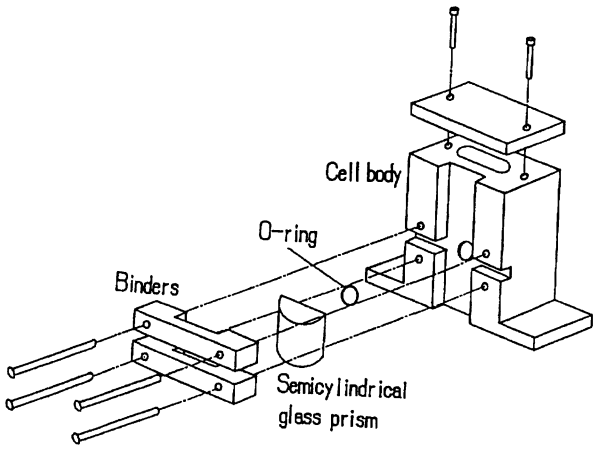

Fig. 2. Internal-reflection cell.

Theoretical

According to a theoretical treatment by Hansen,[16] the reflectivity (R) at an interface where several light-absorbing thin layers are stratified between an incident transparent phase and a final absorbing phase (see Fig. 3) is expressed by

$$1-R=(1/n_1\cos\theta_1)(\sum_i n_i\alpha_i<E^2>_i h_i+n_f\alpha_f<E^2>_f d), \quad (1)$$

where n_i, α_i, and h_i are the refractive index, absorption coefficient, and thickness of the absorbing thin layer i. α_i is related to the extinction coefficient (k_i) by $\alpha_i=4\pi k_i/\lambda$, where λ is the wavelength in vacuum. n_1 and n_f are the refractive indices of the incident and final phases, respectively, and θ_1 is the angle of incidence. $<E^2>_i$ is a normalized time-space average of the light intensity in the layer and $<E^2>_f$ is a normalized time average of the light intensity in the final phase at the final boundary. d is so called the penetration depth in the final phase. $<E^2>_i$, $<E^2>_f$, and d are functions of n's, k's, and h's, and θ_1. In order to analyze the glass-solution interface, we can rewrite Eq. 1 in the proper form for either a two- or three-phase system. As described later, the two-phase system is a model of the case in which the dye molecules uniformly distribute from the interface to the bulk of the solution, whereas the three-phase system corresponds to the case in which the dye molecules are adsorbed by the glass substrate to form an adsorption layer on the glass substrate.

Two-Phase System. In this case, Eq. 1 becomes

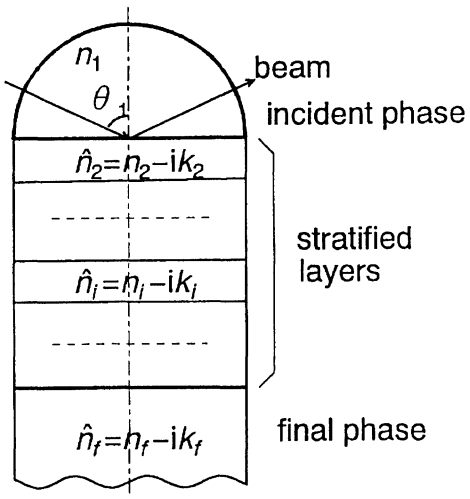

Fig. 3. Interface comprising several stratified thin films. The meanings of the symbols are explained in the text.

a simple form and is expressed by

$$1 - R = (1/n_g \cos\theta_1)(n_s\alpha_s < E^2 >_s d), \quad (2a)$$
$$= 2.303 a b_e c, \quad (2b)$$

where the glass substrate and the solution are represented by suffixes g and s, respectively. a, b_e, and c are the molar absorption coefficient, the effective thickness, and the concentration of the dye. Equation 2b is a central equation of the attenuated total reflection spectroscopy (ATR). (When $R \ll 1$, the left-hand side of Eq. 2, $1-R$, can be approximated by $\log(1/R)$, that is, the reflection absorbance.) Equation 2b has been generally employed in total internal-reflection spectroscopy in which the angle of incidence is greater than the critical angle (θ_c). However, it can be applied to internal-reflection spectroscopy with any angle of incidence from 0° to 90°. Above θ_c, b_e is the optical path concerning the evanescent wave, whereas below θ_c, it is the projection of $1/\alpha_s$ onto the normal to the glass-solution boundary. As described later, a plot of $1-R$ against b_e is more diagnostic than a plot of R against θ_1 for judging whether the adsorption layer is present or not on the glass substrate.

Three-Phase System. In this case, $1-R$ comprises two terms contributed from the thin absorbing film, that is, the adsorption layer and the final solution phase. Namely,

$$1-R = (1/n_g \cos\theta_1)(n_{ad}\alpha_{ad} < E^2 >_{ad} h_{ad} + n_s\alpha_s < E^2 >_s d), \quad (3)$$

where suffix ad denotes the adsorption layer. The purpose of the present work is finally reduced to determining n_{ad}, k_{ad} or α_{ad}, and h_{ad}. However, these parameters appear as their product in Eq. 3. Therefore, each parameter cannot be independently determined unless the remaining parameters have been previously determined by other methods, such as a Kramers–Krönig analysis. In order to determine the product, $P = n_{ad}\alpha_{ad}h_{ad}$, a plot of R against θ_1 was analyzed by curve fitting based on the following approximate expression derived from Eq. 3:

$$1-R \simeq (1/n_g \cos\theta_1)(P\gamma_1 < E^2 >^\circ_{ad} + n_s\alpha_s\gamma_2 < E^2 >^\circ_s d), \quad (4)$$

When the adsorption layer is adequately thin, $<E^2>_{ad}$ in Eq. 3 is controlled by the glass substrate and the solution phase, and is approximated by[17,18]

$$< E^2 >_{ad} \simeq < E^2 >^\circ_{ad}$$
$$= 4n_g^2 \cos^2\theta_1/(n_g \cos\theta_1 + n_s \cos\theta_3)^2 \quad \text{for } \theta_1 < \theta_c,$$
$$= 4n_g^2 \cos^2\theta_1/(n_g^2 - n_s^2) \quad \text{for } \theta_1 > \theta_c, \quad (5)$$

where $\cos\theta_3 = \sqrt{1-(n_g/n_s)^2\sin^2\theta_1}$ from Snell's law. In addition, $<E^2>_s$ can be approximated by $<E^2>^\circ_s$, which is $<E^2>_s$ at an interface without an adsorption layer, that is, the interface in a two-phase system. γ_1 and γ_2 are correction factors for $<E^2>^\circ_{ad}$ and $<E^2>^\circ_s$, respectively, which indicate changes in the $<E^2>$'s caused by the existence of an adsorption layer. It is thus expected that as h_{ad} approaches 0, both γ_1 and γ_2 approach unity. In practice, in order to determine P, it was assumed that $P\gamma_1$ is equal to P, when γ_2 is nearly unity.

Results and Discussion

Interface without Adsorption Layer (Two-Phase System). Figure 4a shows a plot of R against θ_1 for an interface between a glass substrate and a 1.0 mmol dm^{-3} BB aqueous solution. The plot could be fitted to a theoretical curve (the solid curve) calculated from Eq. 2, indicating that BB is not adsorbed by the glass substrate, but is uniformly distributed from the interface to the bulk of the solution. The plot of R against θ_1 was converted into a plot of $1-R$ against b_e (Fig. 4b). This plot shows a straight line through the origin; the slope of the straight line was determined to be 263 cm^{-1}. This value agreed closely with the absorption coefficient determined by conventional transmission spectrometry. These facts confirm that proportionality exists between $1-R$ and b_e in Eq. 2b and that b_e is a valid optical path not only above θ_c but also below θ_c, at which angle total reflection never occurs.

Interface with Adsorption Layer (Three-Phase

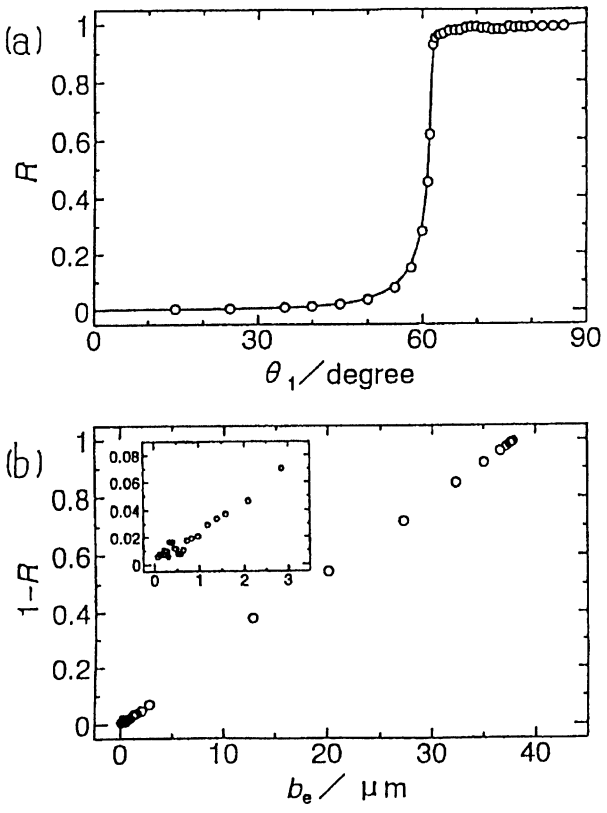

Fig. 4. Plot of R against θ_1 (a) and plot of $1-R$ against b_e (b) for a 1.0 mmol dm^{-3} Brilliant Blue aqueous solution. The solid line shows the theoretical curve calculated from Eq. 2.

Table 1. Diagnoses of the Adsorption and Data from the Curve Fitting for the Interfaces between the Glass Substrate and the Methylene Blue (MB) Solutions Containing Various Kinds of Surfactants[a)]

Surfactants[b)]		n[c)]	Diagnosis[d)]	$P\gamma_1$	γ_2	Residue[e)]
Not contained			Weak	0.00595	0.997	0.00162
	TEAB	2	Weak	0.00473	0.998	0.00120
	OAB	8	Weak	0.00276	1.002	0.00502
Cationic	DEAB	10	Weak	0.01628	0.981	0.00396
	DOAB	12	Weak	0.00593	0.994	0.00257
	CAB	16	No	−0.00180	1.006	0.00185
	ODAB[f)]	18	No	−0.00085	1.005	0.00202
	PTS	1+Ph[g)]	Weak	0.01246	0.989	0.00261
	EBS	2+Ph	Weak	0.00862	0.992	0.00066
	OBS	8+Ph	Strong	0.1631	0.790	0.1345
	DBS	12+Ph	Strong	0.1691	0.773	0.5342
	OS	8	Weak	0.00361	0.999	0.00217
Anionic	DES	10	Weak	0.00791	0.993	0.00045
	DOS	12	Strong	0.1132	0.867	0.09795
	HDS[f)]	16	Strong	0.0703	0.920	0.02651
	SES	2	Weak	0.00807	0.994	0.00195
	SDS	12	Strong	0.1543	0.807	0.1313
	SHDS[f)]	16	Strong	0.1183	0.855	0.03829

a) The concentrations of MB and each surfactant are 1.0 mmol dm^{-3} and 0.2 mmol dm^{-3}. b) TEAB, tetraethylammonium bromide; OAB, octyltrimethylammonium bromide; DEAB, decyltrimethylammonium bromide; DOAB, dodecyltrimethylammonium bromide; CAB, cetyltrimethylammonium bromide; ODAB, octadecyltrimethylammonium bromide; PTS, sodium *p*-toluenesulfonate; EBS, sodium *p*-ethylbenzenesulfonate; OBS, sodium 4-octylbenzenesulfonate; DBS, sodium 4-dodecylbenzenesulfonate; OS, sodium 1-octylsulfonate; DES, sodium 1-decylsulfonate; DOS, sodium 1-dodecylsulfonate; HDS, sodium 1-hexadecylsulfonate; SES, sodium ethylsulfate; SDS, sodium dodecylsulfate; SHDS, sodium hexadecylsulfate. c) Number of carbon in the alkyl group. d) Diagnosis of the adsorption of MB by the plot $1-R$ against b_e. e) Residue for the curve fitting. f) Saturated surfactant solution. g) Ph denotes a phenyl group.

System). Figure 5a is a plot of R against θ_1 for the interface between a glass substrate and a 1.0 mmol dm^{-3} MB aqueous solution. The plot was never fitted to the theoretical curve (the dotted curve in Fig. 5b) calculated from Eq. 2a. This fact implies that MB is adsorbed by the glass substrate to form the adsorption layer. In the same manner as mentioned above, the plot of R against θ_1 was converted into a plot of $1-R$ against b_e, as shown in Fig. 5c. The plot sharply rises in the region of small b_e, but becomes a straight line toward large b_e. Taking into account the fact that the plot for the glass-BB solution interface shows only one straight line through the origin, the behavior of the plot for the glass-MB solution interface clearly proves the existence of an adsorption layer. The slope of the straight line in the region of large b_e was determined to be 99 cm^{-1}, which is different from the absorption coefficient of 106 cm^{-1} obtained from conventional transmission spectrometry. This difference is due to a change in $<E^2>_s$ caused by the adsorption layer. Although the analysis using b_e defined in the two-phase system has revealed the existence of an adsorption layer, no optical parameters of this layer can be extracted from it. Therefore, the plot of R against θ_1 was analyzed by curve fitting based on Eq. 4 for the three-phase system. $P\gamma_1$ and γ_2 obtained are listed in Table 1 together with those for the different interfaces. Because the value of γ_2 (=0.997) is practically unity for this interface, $P\gamma_1$ can be equal to P, that is, $n_{ad}\alpha_{ad}h_{ad}$. Based on the value of $P\gamma_1$ and the optical constants for a monomolecular layer of MB, that is, n_{ad}=1.34 and k_{ad}=0.44,[19)] h_{ad} was calculated to be 0.51 nm. The theoretical curve for h_{ad}=0.51 nm is shown in Fig. 5b together with those for h_{ad}=0.33 nm and 0.69 nm. As can be seen in this figure, the theoretical curve for h_{ad}=0.51 nm fits the plot best. This fact indicates not only that the treatment by Eq. 4 is effective for analyzing the interface with the adsorption layer, but also that the internal-reflection spectrometry is sufficiently sensitive to detect a monomolecular layer. In fact, the thickness of the MB cation was estimated to be 0.40 nm from the van der Waals radius of the methyl group in MB.[20)] Therefore, the agreement between the experimental and estimated values suggests that MB is adsorbed parallel to the glass substrate to form a monomolecular layer. As described later, the experimental value of h_{ad} varied within ca. ±30% in each experiment. In order to obtain a more accurate value of h_{ad}, the goniometer should be improved so as to facilitate a reproducible setting of the angle of incidence and the observation angle of the photodiode detector.

Effect of Surfactant on the Adsorption of MB. The effect of a cationic or anionic surfactant on the

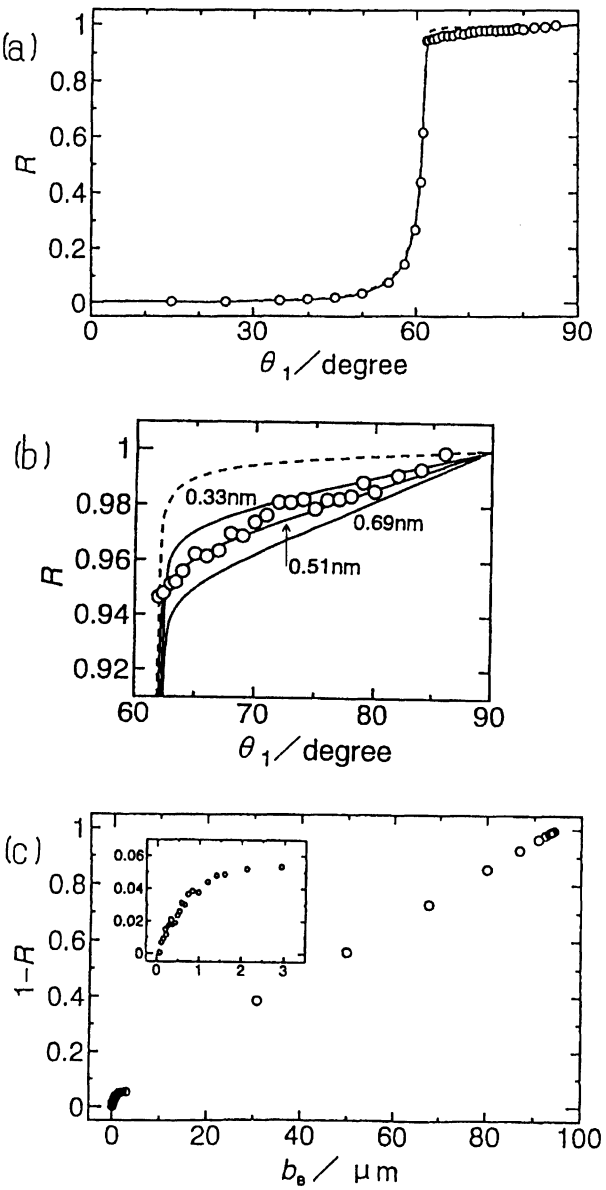

Fig. 5. Plot of R against θ_1 (a) and (b), and plot of $1-R$ against b_e (c) for a 1.0 mmol dm^{-3} Methylene Blue aqueous solution. The dotted and solid lines show the theoretical curves calculated from Eqs. 2 and 4, respectively. Figure 5b is a magnification of Fig. 5a.

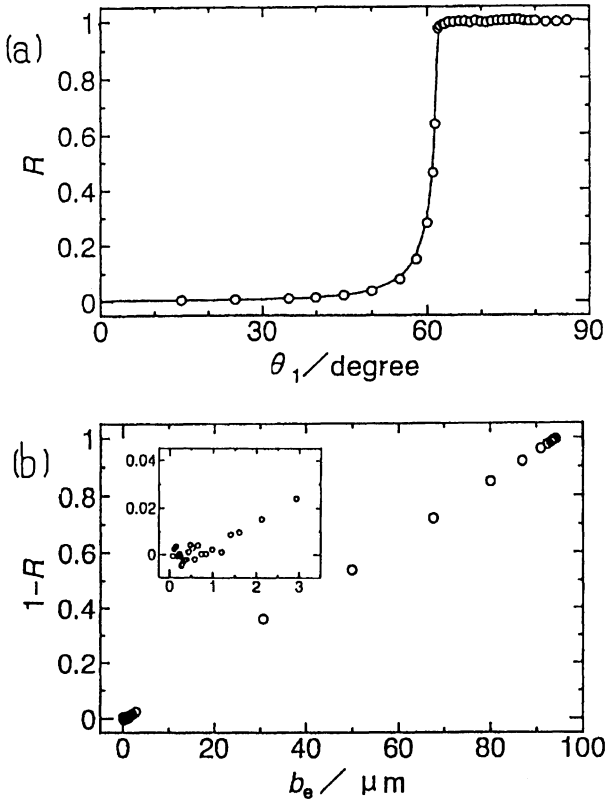

Fig. 6. Plot of R against θ_1 (a) and plot of $1-R$ against b_e (b) for a 1.0 mmol dm^{-3} Methylene Blue aqueous solution containing octadecyltrimethylammonium bromide (ODAB) as a cationic surfactant. The solid line shows the theoretical curve calculated from Eq. 2.

adsorption of MB was investigated. The third column in Table 1 shows the judgment based on the plot of $1-R$ against b_e whether the adsorption layer exists or not. As previously discussed, the proportional relation between $1-R$ and b_e indicates no adsorption, whereas the plot consisting of two curves suggests the occurrence of adsorption. In the case of CAB and ODAB, which are cationic surfactants with long alkyl chains, each plot shows a straight line through the origin, as can be seen in Fig. 6b. It is therefore concluded that CAB and ODAB prevent the adsorption of MB by the glass substrate. Such a cationic surfactant may be more intimately adsorbed by a glass substrate than the MB cation and electrostatically exclude the MB cation from a glass-solution interface. It is next suggested that both the cationic and anionic surfactants with a relatively short alkyl chain do not essentially affect the adsorption of MB, because all of the $P\gamma_1$'s and γ_2's for the MB solutions containing them are similar to that for a solution containing only MB. Namely, the MB cation can be adsorbed by the glass substrate from the solution containing such a surfactant in a similar manner to the case of the solution containing no surfactant. We can therefore assume that the thickness of the adsorption layer is identical for all such solutions. The average thickness of the adsorption layer was determined to be 0.65±0.18 nm, which corresponds to the thickness of the MB cation estimated previously. Fig. 7 shows the plot of R against θ_1 and the plot of $1-R$ against b_e for an MB solution containing SDS, which is an anionic surfactant with a long alkyl chain. Both plots are dramatically changed, indicating that strong adsorption occurs at the interface. Similar dramatic changes were found by adding anionic surfactants with a carbon number of more than 11 in the alkyl chain. The $P\gamma_1$'s for these surfactants are much larger than that for the MB so-

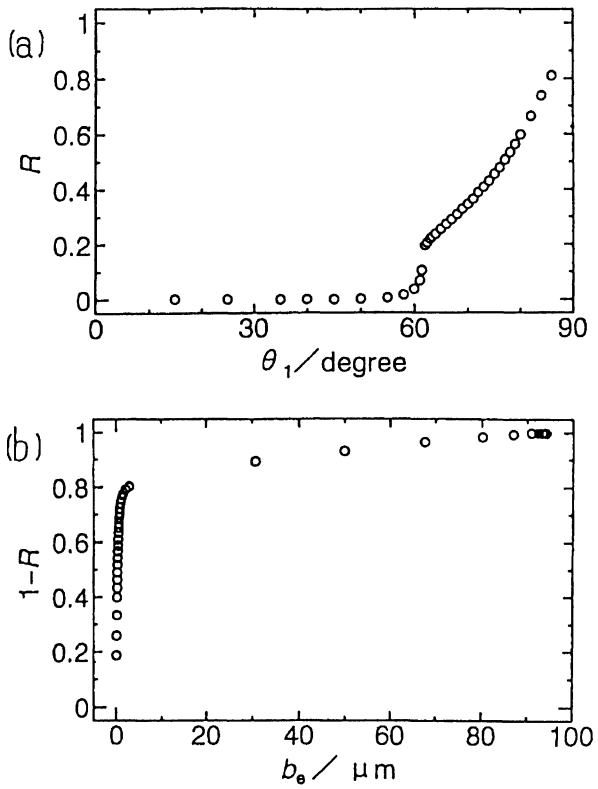

Fig. 7. Plot of R against θ_1 (a) and plot of $1-R$ against b_e (b) for a 1.0 mmol dm^{-3} Methylene Blue aqueous solution containing sodium dodecylsulfate (SDS) as an anionic surfactant.

lution and the γ_2's are markedly different from unity. These results imply that the adsorption layer is considerably thick, compared with a monomolecular layer, and that the surfactants promote the adsorption of MB. Taking into account that the MB cation forms an ion aggregate with an anionic surfactant having a long alkyl chain,[21] the adsorption in this case may be regarded as being a bulky deposition of the ion aggregate onto the glass surface. Equation 4 can no longer be applied to the analysis of the plot of R against θ_1 for the interface with a thick adsorption layer. In fact, the discrepancy in the curve fitting is significantly large, compared with those for the other surfactants. In other words, the plot of R against θ_1 is never fitted to the theoretical curve calculated from Eq. 4 Although it is difficult to analyze the interface with such a thick adsorption layer, a curve-fitting method using a rigorous expression for the three-phase system[7] remains to be developed.

Conclusion

Approximate expressions were derived from the basic theory of internal-reflection spectroscopy in order to analyze a plot of R against θ_1 at a glass-dye solution interface. Curve fitting based on these approximate expressions allowed us to detect a monomolecular layer of the dye adsorbed on the glass substrate. On the other hand, the plot of $1-R$ against b_e, which can be obtained from the plot of R against θ_1, provided a useful diagnosis for readily judging whether an adsorption layer is present or not. Being associated with the curve fitting based on an approximate expression, variable incidence angle internal-reflection spectrometry becomes a prominent method for characterizing *in situ* many solid–liquid interfaces with high spatial resolution on the order of nm.

We are grateful to Dr. Takashi Inagaki of Osaka Kyoiku University for discussing the optical parameters of the thin Methylene Blue film.

This work was partially supported by a Grant-in-Aid for Scientific Research No. 04640553 from the Ministry of Education, Science and Culture.

References

1) "Spectroelectrochemistry," ed by R. J. Gale, Plenum Press, New York (1988).
2) F. M. Mirabella, Jr., and N. J. Harrick, "Internal Reflection Spectroscopy: Review and Supplement," Marcel Dekker, New York (1985).
3) T. Kuwana, "Electroanalytical Chemistry," ed by A. J. Bard, Marcel Dekker, New York (1974), Vol. 7, pp. 2—78.
4) M. J. Bedzyk, G. M. Bommarito, and J. S. Schildkraut, *Phys. Rev. Lett.*, **62**, 1376 (1989).
5) M. J. Bedzyk, G. M. Bommarito, M. Caffrey, and T. L. Penner, *Science*, **248**, 52 (1990).
6) N. J. Harrick, "Internal Reflection Spectroscopy," John Wiley & Sons, New York (1967).
7) W. N. Hansen, "Advances in Electrochemistry and Electrochemical Engineering," ed by P. Delahay and C. W. Tobias, John Wiley & Sons, New York (1973), Vol. 9, pp. 2—60.
8) W. N. Hansen, *ISA Trans.*, **4**, 263 (1965).
9) T. Hinoue, Y. Shimahara, H. Murata, and Y. Yokoyama, *Bunseki Kagaku*, **33**, E459 (1984).
10) T. Hinoue, H. Murata, and Y. Yokoyama, *Anal. Sci.*, **2**, 401 (1986).
11) T. Hinoue, H. Murata, M. Kawabe, and Y. Yokoyama, *Anal. Sci.*, **2**, 407 (1986).
12) T. Hinoue, M. Kawabe, and Y. Yokoyama, *Bull. Chem. Soc. Jpn.*, **60**, 3811 (1987).
13) T. Hirschfeld, *Appl. Spectrosc.*, **31**, 289 (1977).
14) W. M. Reichert, P. S. Suci, J. T. Ives, and J. D. Andrade, *Appl. Spectrosc.*, **41** (1987).
15) X-Z. Wu, T. Kitamori, N. Teramae, and T. Sawada, *Bull. Chem. Soc. Jpn.*, **64**, 2710 (1991).
16) Ref. 7, pp. 29—48.
17) Ref. 6, pp. 50—56 and pp. 281—284.
18) N. J. Harrick, *J. Opt. Soc. Am.*, **55**, 851 (1965).
19) D. A. Higgins, S. K. Byerly, M. B. Abrams, and R. M. Corn, *J. Phys. Chem.*, **95**, 6984 (1991).
20) G. M. Barrow, "Physical Chemistry," McGraw-Hill, New York (1979), p. 529.
21) S. Motomizu, A. Fujiwara, and K. Toei, *Anal. Chem.*, **54**, 392 (1985).